Low-Temperature Study of Photoinduced Energy Transfer from Tryptophan Residues of *Escherichia coli* Alkaline Phosphatase to Bound Terbium

Sanjib Ghosh,[†] Ajay Misra,[§,‡] Andrzej Ozarowski,[§] and August H. Maki*[,§]

Department of Chemistry, Presidency College, 86/1 College Street, Calcutta 700073, India, and the Department of Chemistry, University of California-Davis, One Shields Avenue, Davis, California 95616

Received: April 28, 2003

Low-temperature phosphorescence (LTP) decay measurements have been carried out in wild-type *Escherichia coli* alkaline phosphatase (AP), metal-depleted AP (apoAP), and terbium-substituted AP (TbAP) at 77, 4.2, and 1.2 K. Over this temperature range, Tb emission monitored at 542.4 nm decays with two apparent lifetime components of 16−20 ms and 130−170 ms when TbAP is excited at 280 nm where Tb absorbs negligibly. These lifetimes are orders of magnitude greater than exhibited by $TbCl_3$ at low temperature and by TbAP at room temperature; we attribute this Tb luminescence in TbAP largely to energy transfer from the triplet state of initially excited tryptophan. LTP and ODMR at 1.2 K suggest that Trp^{109} and Trp^{220} have similar environments in AP and in apoAP. Trp^{109} is found to occupy two distinct sites in both AP and apo AP that exhibit resolved ODMR transitions. Comparison of the phosphorescence spectra of AP and TbAP shows clearly that the sensitized Tb emission observed in TbAP is due selectively to energy transfer (ET) from Trp^{109} to Tb and not significantly from Trp^{220}. Evaluation of the results also suggests that ET takes place through space by Dexter's exchange mechanism, where the lowest triplet state of Trp acts as donor and the $^7F_6$ ground state of Tb acts as acceptor. The ratio of the two ET rate constants suggests that two sites of Trp^{109} (possibly those resolved by ODMR) act as donors to either or both metal-binding sites, M2 or M3, rather than one Trp^{109} site transferring energy to Tb at either site M2 or M3.

Introduction

Escherichia coli alkaline phosphatase (AP) is an extensively studied metalloenzyme whose functional form consists of a homodimer with an approximate mass of 94 kDa.[1] AP catalyzes the hydrolysis and trans phosphorylation of a wide variety of phosphate monoesters. The enzymatic reaction proceeds through a covalent serine phosphate intermediate to produce inorganic phosphate and alcohol.[2] Each of the two active sites of the dimeric enzyme contains three metal-binding sites (M1, M2, M3). The M1 and M2 sites are occupied by zinc ions and the M3 site is occupied by a magnesium ion. The three metal ions in each active site form a catalytic metal triad similar to that of phospholipase C from *Bacillus cereus*[3] and P1 nuclease from *Penicillium citrinum*.[4] In contrast to the two Zn^{2+} ions, the Mg^{2+} ion in the M3 site has not been shown to play a direct role in catalysis, although it has been shown to be important for full enzyme activity.[5,6] A recent study suggests that each metal ion assisting in catalysis is a more accurate description of the mechanism of the alkaline phosphatase reaction.[7]

Each AP monomer contains three tryptophan (Trp) residues at positions 109, 220, and 268. AP has received much attention because of the fact that it emits room-temperature Trp phosphorescence (RTP)[8] having a lifetime of ca. 2 s, the longest thus far reported.[9] The long-lived RTP has been assigned to the Trp 109[10−13] that is buried deep in the hydrophobic core of AP. Recent time-resolved studies in AP with Tb^{3+} substitution at the metal sites (TbAP) provided strong evidence that at room temperature the time evolution of AP-bound Tb emission is determined predominantly by energy transfer (ET) from the triplet state of Trp^{109} to Tb^{3+}, followed by Tb^{3+} decay.[14] An earlier ET study[15] in the same system, however, suggests that enhanced emission of Tb^{3+} is sensitized by the lowest singlet state of Trp^{109}.

The nature of the ET mechanism that leads to enhanced emission in Tb-substituted metalloenzymes is not yet fully established. In some Tb metalloenzymes, ET has been demonstrated to proceed by long-range nonradiative energy transfer from protein aromatic singlet states.[16,17] At shorter distances, a Dexter[18] exchange mechanism has been suggested.[19] Rare earth sensitization by aromatic triplet donors in nonbiological systems has been known for some time,[20,21] and quenching of Tb emission by dissolved O_2 strongly suggests the involvement of triplet state donors.[22,23] The presence of an O_2-dependent rise in Tb luminescence following pulsed excitation has been presented as evidence for a triplet state donor in TbAP[14] and in Tb elastase.[24] We undertook this study of the AP system at low temperature to help resolve the nature of protein ET to Tb in TbAP.

Although only relatively few Trp residues (those that are located in buried, rigid local environments) in proteins can be studied readily using RTP, nearly all proteins containing Trp residues emit phosphorescence at low temperature. Origins of individual sites often can be resolved because of the relatively narrow emission bands that characterize Trp low-temperature phosphorescence (LTP). The narrowness of the LTP bands, in contrast with the poorly resolved Trp fluorescence, is attributed to the smaller excited-state dipole moment change in the case of the triplet.[25] The LTP of Trp residues buried in hydrophobic

* To whom correspondence should be addressed. Tel: 530-752-6471. Fax: 530-752-8995. E-mail: maki@indigo.ucdavis.edu.
[†] Presidency College.
[§] University of California-Davis.
[‡] Present address: Department of Chemistry, R.K.M.V.C. College, Rahara, Calcutta-70018, India.

10.1021/jp030522b CCC: $25.00
Published on Web 09/11/2003

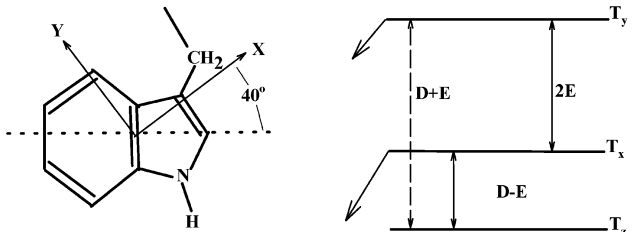

Figure 1. Structure of the indole chromophore of Trp showing the orientation of the zfs principal axes and the zero-field energy level diagram. The prominent ODMR transitions between triplet sublevels, T_i, are indicated with solid double-headed arrows, while the transition observed using EEDOR is labeled with the dashed double-headed arrow. The radiative sublevels carry single headed arrows. $k_x^r > k_y^r$, where k_x^r and k_y^r are the radiative rate constants for the sublevels *x* and *y*, respectively, while the *z* sublevel is not radiative.

regions within proteins is generally red-shifted relative to solvent-exposed residues, and it is better resolved since buried environments are usually highly structured, i.e., homogeneous.[26] Specific interactions with polar residues, however, can result in blue-shifted origins for buried Trps.[27,28]

Optically detected magnetic resonance (ODMR) studies carried out on the excited triplet state of Trp residues in proteins[29−32] indicate that the bandwidth of the ODMR signals correlates well with the homogeneity of the local environment. Buried residues in homogeneous protein environments yield narrow ODMR signals. In addition, red-shifted phosphorescence origins correlate with reduced values of D − E, where D and E are the triplet state zero-field-splitting (zfs) parameters.[33] The structure of the Trp side chain with the location of the zfs principal axes is shown in Figure 1, along with the zero-field energy level diagram.

Earlier preliminary studies[34] of the phosphorescence and zero-field ODMR of the Trp residues in wild-type AP, W220Y AP, and the TbAP showed that each Trp can be resolved optically. Trp^{109}, known from the earlier work[10,11] to be the source of RTP, emits a highly resolved LTP spectrum and has the narrowest ODMR bands observed thus far from any protein site, revealing a uniquely homogeneous local environment. The decay kinetics of Trp^{109} at 1.2 K reveals that the major triplet population (70%) undergoes inefficient crystal-like spin−lattice relaxation (slr) by direct interaction with the lattice phonons, the remainder being relaxed efficiently by local disorder modes.[34] The latter population is smaller than is typical for protein sites, suggesting an unusual degree of local rigidity that is consistent[35] with the long-lived RTP. Trp^{220} emits a broader LTP spectrum originating to the blue of Trp^{109}, and it exhibits typically broad ODMR bands consistent with local heterogeneity. The LTP of Trp^{268} has an ill-defined origin blue-shifted relative to Trp^{220} and ODMR frequencies consistent with a greater degree of solvent exposure. Trp^{268} has noticeable dispersion of its decay kinetics, consistent with quenching at the triplet level by a nearby disulfide residue.[36]

These results[34] along with the conflicting earlier ET studies on TbAP at room temperature[14,15] prompted us to investigate the ET in detail in the low-temperature region (77−1.2 K). The present work has been carried out primarily to address the following:

(1) Does metal removal in AP or Tb^{3+} substitution in apoAP perturb the protein structure as evidenced by studying the environment of Trp residues by phosphorescence and ODMR spectroscopy?

(2) Can the role of Trp^{109} as donor in the ET process be confirmed, and do other Trp residues take part?

(3) Is the lowest singlet state (S_1) or the lowest triplet state (T_1) the major energy donor at low temperature, and what is the dominant mechanism of ET at low temperature?

(4) What are the ET rates at various temperatures in the low-temperature region (77, 4.2, and 1.2 K) and how do they compare with the ET rates observed at room temperature?[14]

To shed some light on these questions, we report here LTP and zfs parameters of the lowest triplet state in zero magnetic field and triplet sublevel dynamics of Trp residues in AP, apoAP, and TbAP. In addition, we report decay kinetics monitoring the emissions of Tyr, Trp, and Tb^{3+} in TbAP at low temperature. Decay kinetics of free $TbCl_3$ in the same medium at low temperature also was studied as a control. These results have been evaluated to find a plausible mechanism of ET in TbAP at low temperature.

Experimental Section

Materials. AP was a product of Sigma (type III, chromatographically purified suspension in 2.5 M $(NH_4)_2SO_4$, activity 43.7 u/mg of protein). AP was exchanged into 100 mM Tris buffer containing, in addition, 1mM Na_2HPO_4, 0.1 mM $MgCl_2$, and 0.1 mM $ZnCl_2$, using Centricon 30 filter centrifugation at 5000g and 4 °C. Ethylene glycol (EG) was added to 30 vol % as cryoprotectant for low-temperature measurements. The final concentration of AP was about 2.5×10^{-4} M in our samples. AP with terbium substitution at the metal sites (TbAP) was obtained by first preparing metal-depleted AP (apoAP) following the method of Bosron et al.[2] using the metal chelator, 8-hydroxyquinoline-5-sulfonic acid (Aldrich). ApoAP was washed with three exchanges of metal-free tris(hydroxymethyl)aminomethane (Tris) buffer. Tris buffer containing 10 mM $TbCl_3$ was added, and the solution was incubated for 30 min prior to washing the TbAP twice with metal-free buffer. The entire procedure was carried out by refrigerated (4 °C) centrifugation at 5000g using a Centricon 30 filter.

Methods. Samples (30−50 μL) were contained in a 2-mm inside diameter Suprasil quartz tube held inside a copper helix terminating a coaxial stainless steel microwave transmission line. This structure was inserted into a stainless steel dewar with quartz optical windows in which the sample temperature could be held at 77 K (boiling N_2 temperature), 4.2 K (immersed in boiling He), or 1.2 K (immersed in vacuum-pumped He) for LTP and zero-field ODMR measurements. The sample was excited by a 100 W high-pressure Hg lamp whose output was filtered through a 0.1 m monochromator. Glass filters were used as required to further limit the excitation band. Phosphorescence was observed through a rotating sector with a delay period of ca. 1 ms and monitored through a 1 m monochromator with a dispersion of 0.8 nm/mm. Details of the phosphorescence and ODMR spectrometer that employs photon counting to enhance sensitivity has been given previously.[37,38] Center frequencies (ν_0) and bandwidths ($\nu_{1/2}$, half the width at half-maximum intensity, hwhm) of the ODMR bands (assumed Gaussian shape) were determined by analysis of phosphorescence responses, obtained by sweeping the microwave frequency slowly through the zero-field resonance band, using algorithms developed previously for steady-state ODMR[37] and for delayed ODMR.[39] These algorithms corrected for band distortions caused by rapid passage effects. The highest-frequency (D + E) ODMR band was observed using electron−electron double resonance (EEDOR),[30] simultaneously saturating the low-frequency (D − E) band. The individual kinetic parameters of the triplet state sublevels were obtained by global analysis of microwave-induced delayed phosphorescence (MIDP)[40] data sets using a

TABLE 1: Triplet State Spectroscopic Properties of Trp Residues in *E. coli* AP and ApoAP[a]

	$\lambda_{0,0}$ (nm)[b]		D − E		2 E		D + E[c]		D	E
sample			ν_0 (GHz)	$\nu_{1/2}$ (MHz)	ν_0 (GHz)	$\nu_{1/2}$ (MHz)	ν_0 (GHz)	$\nu_{1/2}$ (MHz)	(GHz)	(GHz)
AP Trp^{109}	414.5	site I	1.583(3)	7.0 (5)	2.768(8)	18 (1)	4.344(1)	13 (1)	2.964	1.382
		site II	1.61(2)	11 (1)	2.704(5)	20 (1)			2.96	1.35
AP Trp^{220}	411.4		1.675(5)	43 (2)	2.63(6)	94 (12)	4.29(1)	53 (3)	2.98	1.31
ApoAP Trp^{109}	413.7	site I	1.588(3)	7.0 (5)	2.80(4)	20 (2)			2.99	1.40
		site II	1.625(3)	12 (2)	2.70(5)	23 (2)			2.98	1.35
Apo AP, Trp^{220}	411.1		1.675(5)	43 (2)	2.635(9)	90 (12)			2.99	1.32

[a] Proteins are ca. 2.5×10^{-4} M in 30% (v/v) EG-Tris buffer. Standard deviation in the final digit is in parentheses. [b] 0,0-Band peak wavelength. [c] ODMR band observed using EEDOR.

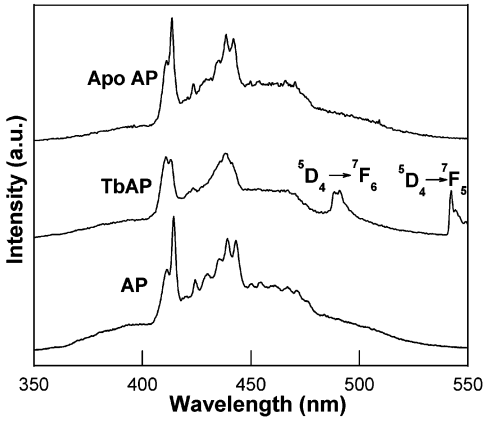

Figure 2. Phosphorescence spectra of apoAP, TbAP, and AP. Samples (concentration $\sim 2.5 \times 10^{-4}$ M) are dissolved in 30% (v/v) EG-Tris buffer glass at 4.2 K. They are excited at 280 nm, and the emission bandwidth is 1 nm. The sample is viewed through a rotating can phosphoroscope with delay time of 1 ms. Two sensitized terbium emission bands are indicated in the TbAP spectrum. Phosphorescence intensity is normalized at 411.4 nm.

previously described procedure.[38] These were comprised of the sublevel decay constants, k_i, the slr rate constants, W_{ij}, the relative intersystem crossing (isc) rates, P_i, and the relative radiative rate constants, R_{ij} ($= k_i^r/k_j^r$). $i,j = x, y, z$ labeled the principal zero-field magnetic axes of the indole chromophore of Trp,[41] shown in Figure 1. Decay kinetics were obtained using a mechanical shutter in the excitation path with a closing time of 1 ms. Trp LTP lifetimes at 4.2 K were obtained in the following manner. The decay of tyrosine (Tyr) LTP was recorded with wavelength selection to the blue of the Trp emission. This decay was weighted by its contribution to the steady-state phosphorescence intensity at the 0,0-band peak of Trp and subtracted from the overall LTP decay at this wavelength. The tyrosine contribution was readily assessed since its phosphorescence presented a broad, unstructured background in contrast with the highly resolved bands of Trp. The residual LTP, attributed to Trp, was fitted to a single exponential using least-squares minimization. Tryptophan LTP decay at 4.2 and 77 K is known to be exponential over at least 3 decades, while Tyr decays nonexponentially at these temperatures.[30,42] Tb^{3+} luminescence was monitored at its 542.4 nm peak with narrow band-pass to minimize Trp background phosphorescence. Excitation is sufficiently long (ca. 15 s for Trp and Tyr and ca. 2 s for Tb) to ensure the attainment of steady-state populations prior to observing the decay kinetics.

Results

Phosphorescence Spectra. Figure 2 shows the phosphorescence spectra of AP, TbAP, and apoAP at 4.2 K. AP exhibits overlapping phosphorescence spectra from Trp residues 220 and 109 with resolved 0,0-bands peaking at 411.4 and 414.5 nm (Table 1). The spectrum of W220Y AP lacks the broader 0,0-band at 411.4 nm (allowing the assignment of this band to Trp^{220}), and reveals a weak 0,0-band at ca. 408 nm that has been assigned to Trp^{268}.[34] An unstructured underlying emission originating near 350 nm observed in the spectrum is assigned to Tyr residues. The spectrum of TbAP shows that the phosphorescence assigned to Trp^{109} is severely quenched relative to that of Trp^{220}, and concomitant structured emission bands from Tb^{3+} appear. The Tb^{3+} emission is sensitized by ET; direct excitation of Tb^{3+} at 280 nm is negligible.[14] The background Tyr emission is partially quenched in the TbAP and apoAP spectra.

ApoAP shows 0,0-bands at 413.3 and 411.1 nm. The 413.3 nm band is assigned to Trp^{109} and the 411.1 nm band to Trp^{220} by comparison with AP. A small blue shift of Trp^{109} in both apoAP and TbAP relative to AP is evident. LTP spectra of AP, TbAP, and apoAP obtained at 1.2 K are presented in Figure 3a at higher resolution, while the sensitized Tb^{3+} $^5D_4 \rightarrow {}^7F_6$, $^5D_4 \rightarrow {}^7F_5$, and $^5D_4 \rightarrow {}^7F_4$ transitions in TbAP are shown separately in Figure 3b. The apparent width of the Trp^{109} 0,0-band in the spectrum of AP and apoAP is only 40 cm^{-1}, hwhm, in contrast with the 411.4 nm 0,0-band of Trp^{220} that has a more typical value (for protein sites) of 150 cm^{-1}. These results, and those to be presented below, indicate that the metal-depleted protein has a highly homogeneous environment for Trp^{109} similar to that observed in the AP.

Optically Detected Magnetic Resonance. The slow passage ODMR transitions that are found in the D − E frequency region of Trp are shown in Figure 4. The D − E transition occurs between the T_z (longest lived and nonradiative) and T_x (shortest lived and most radiative) sublevels and is (without a known exception to date) the narrowest of the three ODMR bands of Trp.[29,30] The Trp^{109} ODMR bands are found both in AP and apoAP by optically selecting the 414.5 nm band and 413.7 nm 0,0-band, respectively, with slits set for a narrow band-pass. The unusually narrow ODMR band has a doublet structure in both the samples. A far broader ODMR band, assigned to Trp^{220}, is observed in AP and apoAP by monitoring the LTP at 411.4 and 411.1 nm, respectively. ODMR bands were also observed from these residues in the 2E region and from Trp^{109} and Trp^{220} in the D + E region using EEDOR. These data were analyzed using algorithms described earlier;[37,39] the zfs data are reported in Table 1. ODMR signals of Tyr (not reported) occur in different frequency ranges and do not interfere with those of Trp.[30,31] In contrast with AP and apoAP, the LTP decay kinetics of TbAP at 1.2 K are indistinguishable from those measured at 4.2 K, and no ODMR signals are detected at 1.2 K. Bound Tb apparently induces efficient slr in the triplet states so that the spin alignment at 1.2 K is lost. The mechanism is likely to involve interaction between the triplet states of Trp and a fluctuating magnetic field set up by the $J = 6$ ground state of Tb^{3+} interacting with disorder modes of the glass−protein matrix.[43−45]

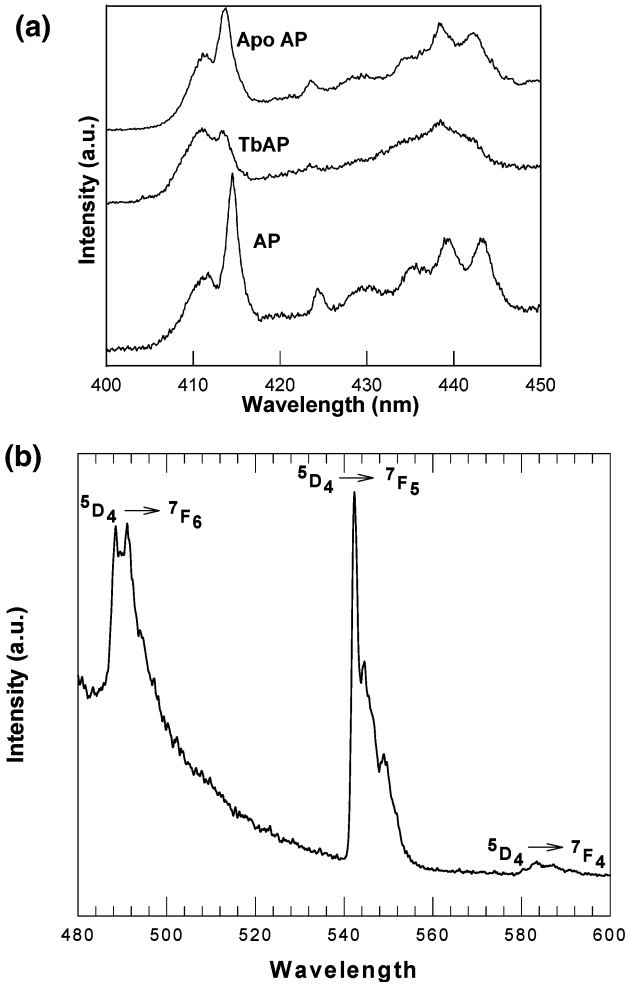

Figure 3. (a) High-resolution phosphorescence spectra of apoAP, TbAP, and AP at 1.2 K. Samples are as described in the Figure 2 caption. Samples are excited at 280 nm and viewed through the phosphoroscope using 0.5 nm emission bandwidth. (b) Emission bands of Tb^{3+} in TbAP at 1.2 K. Sample is same as described in the Figure 2 caption. $\lambda_{exc} = 280$ nm, emission band-pass = 0.5 nm.

Decay Measurements. Table 2 shows the analysis of the luminescence decay measurements of TbAP, AP, apoAP, and $TbCl_3$. For TbAP, we measured the decay at 542.4 nm, the sensitized emission ($^5D_4 \rightarrow {}^7F_5$) of Tb^{3+}, since the band at 480 nm overlaps with Trp emission. The ET kinetics of TbAP are described by the scheme

$$\text{Trp*—Tb} \xrightarrow{-k_{ET}} \text{Trp—Tb*} \quad (1)$$

$$\text{Trp*—Tb} \xrightarrow{-k_{d}} \text{Trp—Tb} \quad (2)$$

$$\text{Trp—Tb*} \xrightarrow{-k_{a}} \text{Trp—Tb} \quad (3)$$

where k_{ET} is the rate constant for ET from the excited state of the tryptophan donor, Trp*, k_d is the rate constant for the normal decay of Trp* at low temperature, and k_a is the decay constant of excited Tb^{3+}, Tb*. This scheme leads to the differential equations

$$d\text{Trp*}/dt = -(k_d + k_{ET})\text{Trp*} = -\lambda_d \text{Trp*} \quad (4)$$

and

$$d\text{Tb*}/dt = k_{ET}\text{Trp*} - k_a\text{Tb*} \quad (5)$$

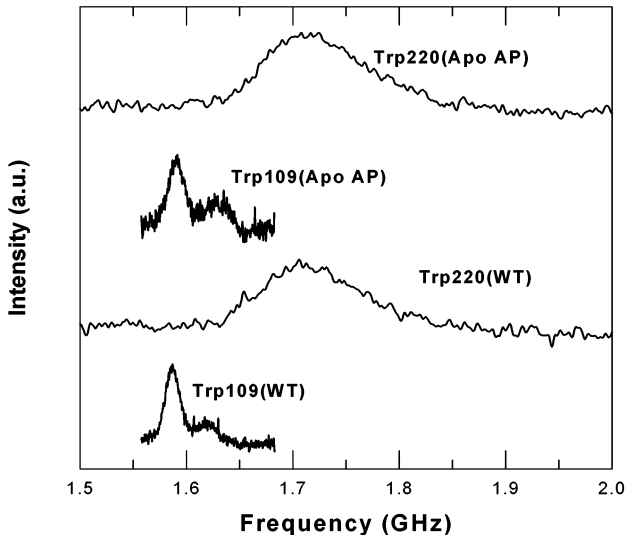

Figure 4. Steady-state slow passage D − E ODMR transition of Trp in AP and apoAP at 1.2 K. In AP, the Trp^{109} band is observed monitoring the 0,0-band at 414.5 nm using 0.5 nm bandwidth while the Trp^{220} is observed monitoring the 0,0-band at 411.4 nm using 1 nm bandwidth. In apoAP, Trp^{109} band is observed monitoring the 0,0-band at 413.7 nm using 0.5 nm bandwidth while Trp^{220} is observed monitoring the (0,0)-band at 411.1 nm using 1 nm bandwidth. The sweep rate is 2.67 MHz/s for Trp^{109} and 4.5 MHz/s for Trp^{220}. Signal averaging is employed for 40 cycles.

TABLE 2: Results of Analysis of Decay Measurement[a]

sample	temp (K)	λ_{exc} (nm)[b]	λ_{obs} (nm)[b]	lifetime (ms)[c]	k_{ET} (s^{-1})[d]
TbAP	77	280	542.4	16.2 (44) 169 (56)	61.4, 5.7
TbAP	4.2	280	542.4	20 (39) 133 (61)	49.3, 7.2
TbAP	1.2	280	542.4	19 (26) 128 (74)	52.4, 7.6
AP Trp^{109}	1.2	280	414.5	5900	
apo AP Trp^{109}	1.2	280	413.7	5950	
$Tb(NO_3)_3$	77	280	542.4	1.61 ± 0.03[e]	
$TbCl_3$				<2	
$TbCl_3$	1.2	280	542.4	3	

[a] Sample conditions are as given in the Figure 2 caption. [b] λ_{exc} and λ_{obs} are the excitation and observation wavelengths, respectively. [c] Numbers in parentheses are the relative amplitudes (in %) of the lifetime components resulting from a biexponential least-squares analysis. [d] The estimated error is ±10%. [e] Reference 51.

The solution for Tb*(t) is

$$\text{Tb*}(t) = k_{ET}\text{Trp*}_0 \exp(-\lambda_d t)/(k_a - \lambda_d) + C \exp(-k_a t) \quad (6)$$

where Trp*_0 is the initial donor concentration. The integration constant, C, is evaluated with the aid of eq 5 with $d\text{Tb*}/dt = 0$ at $t = 0$ since we then have a photostationary state. Also, since the Trp^{109} phosphorescence is quenched at low temperature, $k_d \ll k_{ET}$, we can set λ_d equal to k_{ET}. The final result is

$$\text{Tb*}(t) = \text{Tb*}_0[k_a \exp(-k_{ET}t) - k_{ET} \exp(-k_a t)]/(k_a - k_{ET}) \quad (7)$$

where Tb*_0 is the initial population of the acceptor. Equation 7 describes the sum of a decreasing and increasing exponential; both would be observed if k_a and k_{ET} were of similar size. Clearly this is not the case, since we observe only a (apparently biexponential) decrease in Tb^{3+} emission. The decay constant that characterizes a decreasing exponential is the *smaller* of k_a

TABLE 3: Kinetic and Radiative Parameters of the Trp[109] and Trp[220] Residues in AP and Trp[109] in ApoAP[a]

sample/ residue	τ (s)[b]	k_x (s^{-1})	k_y (s^{-1})	k_z (s^{-1})	R_{yx}	R_{zx}	W_{xy} (s^{-1})	W_{xz} (s^{-1})	W_{yz} (s^{-1})	P_x	P_y	P_z
AP Trp109	5.90	0.39(1)	0.106(7)	0.004(5)	0.00(1)	0.00(1)	0.033(5)	0.030(8)	0.0402(9)	0.60	0.30	0.10
AP Trp220	5.95	0.390(9)	0.113(4)	0.000(3)	0.065(6)	0.036(9)	0.004(3)	0.045(4)	0.0402(4)	0.43	0.48	0.09
ApoAP Trp109	5.95	0.38(2)	0.11(1)	0.000(8)	0.00(2)	0.000(8)	0.032(9)	0.03(1)	0.058(1)	0.60	0.30	0.10

[a] All measurements are made monitoring the 0,0-band of the Trp residue using MIDP with these data obtained at 1.2 K. The estimated error in the last digit is given in the parentheses while the estimated error of P_x and P_y is $\pm$ 0.03. [b] τ is the lifetime component attributed to Trp, obtained by elimination of the tyrosine contribution. This measurement was made at 4.2 K.

and k_{ET}. Since the observed decay constants are orders of magnitude smaller than is reasonable for k_a, we assign the decay kinetics to k_{ET} and their nonexponential nature to sample heterogeneity (see below).

Triplet State Sublevel Decay Behavior of Trp Residues. Global analysis of MIDP data sets was carried out,[38] yielding the kinetic data reported in Table 3. The microwave sweep was restricted to the ODMR band of a residue, and the decay was monitored in its 0,0-band (reported in Table 1) to select the residue and to minimize signal contamination.

Discussion

Phosphorescence Spectra and ET. The 0,0-bands of Trp[109] and Trp[220] phosphorescence appear at 414.5 and 411.4 nm, respectively, in AP. The Trp[268] phosphorescence is extremely weak in AP and in apoAP.[34] It is probably quenched by a nearby disulfide residue, Cys[286]−Cys[336].[7] For apoAP, the 0,0-bands of Trp[109] and Trp[220] appear at 413.7 and 411.1 nm, respectively (Table 1). The band positions and their widths indicate that the Trp residues 109 and 220 have similar environments in apoAP compared with those in AP. Although the RTP of AP is lost upon removal of metal ions,[15] indicating a loss of rigidity, our results suggest that apoAP folds at reduced temperature into a structure similar to native AP. Comparison of the phosphorescence spectra of AP, apoAP, and TbAP (Figure 2) clearly confirms that Trp[109] is primarily involved in ET to bound Tb. The intensity of Trp[220] phosphorescence is not affected in TbAP compared to that in AP and apoAP. Catalytic activity of AP requires the presence of Zn^{2+} at metal-binding site M1,[46] while Zn^{2+} and Mg^{2+} bound at M2 and M3, respectively, could have either a structural[46] or cocatalytic[7,47] function. It is difficult to predict which of these metal sites contain Tb^{3+} in our sample of TbAP, but previous work[14] demonstrates that energy transfer to Tb^{3+} occurs with a single bound Tb^{3+} per AP monomer. Trp[109] is the closest Trp residue to the metal sites. The distances between its indole ring center (midpoint of the $C_\delta-C_\epsilon$ bond) and M1, M2, M3 are 13.7, 9.7, and 9.3 Å, respectively. These distances are obtained from atomic coordinates deposited in the Brookhaven Protein Data Bank.[7] It is likely that the weak 0,0-band of Trp[109] that is observed in the TbAP sample (Figures 2 and 3a) reveals the presence of a small amount of apoAP that has not bound Tb^{3+}.

The contribution of Tyr phosphorescence (the broad background emission underlying Trp phosphorescence) is reduced in TbAP compared to that in AP. It is tempting to suggest that Tyr[84] that lies 12.4, 12.1, and 11.4 **Å** from the M1, M2, and M3 sites, respectively, might contribute to ET to Tb. However, it is noted that the Tyr phosphorescence in the total phosphorescence spectra of apoAP is also reduced to some extent compared to that in AP. Thus, it is difficult to determine whether Tyr also takes part in the ET process to Tb^{3+}.

ODMR Transitions in Zero Magnetic Field. The ODMR signals for the D − E transition of Trp[109] in both AP and apoAP appear as two bands, labeled site I (major) and site II (minor) (Figure 4 and Table 1). The splitting, ca. 30 MHz, is too large to ascribe to ^{14}N quadrupole and hyperfine interactions in zero field.[48] These two sites are thus assumed to originate from distinct AP conformations that involve slightly different Trp[109] interactions with the surrounding protein matrix. These conformations appear to survive unaltered in the metal-depleted apoAP. However, the sites are too subtly different to be resolved in the phosphorescence spectra (Figures 2 and 3a). The presence of two sites does not depend on the metal complement since they occur in both AP and apoAP. The ODMR bands of Trp[109] in site I are 2−3 times narrower than any thus far observed in proteins (Figure 4, Table 1). Trp[109], site II, although not as homogeneous as site I, nonetheless is extremely well defined. It is notable that the RTP of AP has been found to decay nonexponentially[49] and that the analysis by the maximum entropy method[50] produced two distinct lifetime peaks of 1920 ms (major) and 380 ms (minor). This behavior was attributed to the existence of at least two discrete structures that are unable to interconvert on the RTP time scale. We suggest that the nonexponential RTP decay could arise from the conformations that are resolved as site I and site II in the ODMR spectra (Figure 4). Furthermore, a comparison of the zfs parameters D and E and the width of the ODMR transitions of Trp[109] and Trp[220] in apoAP and AP (Table 1) suggests that at low temperature, apoAP provides similar environments for both residues as does AP.

Sublevel Decay Kinetics of Trp[109] in ApoAP. The sublevel decay kinetics and populating rates of Trp[109] in apoAP presented in Table 3 are similar to those found for Trp[109] in AP. These data, along with the phosphorescence spectra and zfs parameters, clearly suggest a similar environment for Trp[109] in AP and apoAP.

ET Rate Constants. The decay, monitoring the Tb^{3+} emission at 542.4 nm in the TbAP sample at various temperatures, is fitted well with two exponential components (Table 2) of ~20 ms and ~150 ms that show no great temperature dependence in the 1.2−77 K range. The lifetime of the excited $^5D_4$ state of Tb^{3+} in $TbCl_3$ at 1.2 K was found to be 2−3 ms. At 77 K, the lifetime is less than 2 ms (Table 3). The lifetime reported for pure $Tb(NO_3)_3$ at 77 K is ca. 1.4 ms.[51] The Tb^{3+} luminescence lifetime increases upon chelation with nonproton-containing ligands. Its radiative quantum yield is difficult to measure with accuracy because of its weak absorbance and the lack of an appropriate standard. However, a lifetime of 2.50 ms has been measured for Tb^{3+} bound to octopus calmodulin in D_2O solvent that is reduced to 1.20 ms in H_2O.[52] Assuming a 100% quantum yield in D_2O leads to good agreement with the calculated tyrosine to Tb^{3+} ET efficiency in octopus calmodulin.[17] Thus, the radiative lifetime of excited Tb^{3+} should not exceed ca. 3 ms; we conclude, therefore, that the far longer lifetimes observed for Tb^{3+} decay in TbAP reflects ET rate constants.

The ET rate constants calculated from these lifetimes are ~50 s^{-1} and ~7 s^{-1} at low temperatures (Table 2). At room

temperature, the reported ET rate constants are much larger: 360 and 120 s^{-1} for a deoxygenated sample and 470 and 130 s^{-1} for an oxygenated sample of TbAP.[14] The larger ET rates at room temperature could well be due to thermal fluctuations that modulate the distance and relative orientations of donor and acceptor. We monitored the 4.2 K phosphorescence decay of TbAP at 394, 411.1, and 413.7 nm. The decay is nonexponential in each case, with kinetics consistent with unperturbed Tyr at 394 nm and unperturbed Trp and Tyr at the longer wavelengths. No shorter components could be detected. Given the ET rate constants deduced from the Tb luminescence, decay of donor triplet states should occur overwhelmingly via ET.

ET Mechanism. Considering the possibility of a dipole−dipole Förster type ET mechanism,[53] one starts with a S_1 or T_1 excitation of the Trp site and with a $^7F_6$ ground state of the Tb^{3+} site. For Förster ET to occur between the sites, the S_1 or T_1 state of Trp (donor, D) must make a local dipole transition to its S_0 state while the Tb^{3+} (acceptor, A) must be excited from $^7F_6$ to some excited state by a local dipole transition. Both local transitions must be dipole-allowed because the Förster mechanism employs the dipole−dipole interaction in the multipole expansion of the intersite Coulombic interaction. The mechanism in this case does not involve the S_1 state of Trp, since our experimental results are consistent with energy transfer from a long-lived donor state. If the T_1 state of Trp is the initial state in the Förster transfer, then the local dipole transition in Trp is to be accompanied by an intensity borrowing from local singlet states. This added spin−orbit perturbation increases the order of the perturbation theory by at least one order beyond "pure" Förster theory. For the rare earth ion site, a Förster mechanism demands that the $^7F_6$ state must be excited by an allowed dipole transition, which means that the local transition cannot be an f−f transition because of Laporte's selection rule (for local centrosymmetry, allowed transitions involve a change with respect to the inversion operator). The CT state arising from a putative counteranion, i.e., Cl^{-1}, could be involved in intensity borrowing at the Tb^{3+} site. Thus, in order that the Förster mechanism be operative it must actually be an augmented Förster process, involving at least two local intensity-borrowing transitions, one at each site. The perturbation order is increased by at least two, which, if the perturbation expansions are meaningful, implies that the order of smallness may be 2 orders of magnitude down from a pure Förster mechanism. Schlyer et al.[14] made a calculation for TbAP using Förster's mechanism and found that $k_{ET} = 3.6 \times 10^{-4}\ s^{-1}$ at room temperature, taking the donor−acceptor distance as 9.55 Å, an average of M2 and M3, the two nearest metal-binding sites, and the orientation factor as 2/3.

It may then be concluded that ET involves Dexter's exchange mechanism[18] using either of the following routes:

(a) ET could originate from the lowest excited singlet state of the Trp^{109} and terminate in the rare earth ion ^5D terms. The possibility of ET by exchange mechanism from the lowest excited singlet state of Trp to the rare earth ion state is spin forbidden, and is thus not likely to be important.[54] Also, this mechanism can be ruled out by considering the kinetics of ET, as discussed earlier.

(b) The other possible route of ET originates in the T_1 state of Trp^{109}. This process is spin allowed for many of the excited terms of the $4f^6$ configuration of Tb^{3+}, including the ^5D terms.[54] The decay analysis presented in Table 2 and selective phosphorescence quenching (Figure 3a) confirm the involvement of the T_1 state of Trp^{109}.

The Dexter exchange mechanism using the T_1 state of Trp in ET to Tb^{3+} has been suggested for the Tb-elastase system.[24] Kirk et al. have reported a through-bond exchange mechanism involving the T_1 state of indole in Tb-indolyl−EDTA complexes.[54]

According to Dexter's[18] relation for a short-range exchange interaction, the electronic energy transfer rate constant, k_{ET}, is given by

$$k_{ET} = (2\pi/\hbar)Z^2 J_E \tag{8}$$

where $\hbar$ is Planck's constant, J_E is the integral of spectral overlap between donor emission and acceptor absorption spectra given by

$$J_E = \int_o^\infty F_D(\nu)\epsilon_A(\nu)\, d\nu \tag{9}$$

where F_D and ϵ_A are the normalized donor emission and acceptor absorption spectra, respectively, and Z is the exchange integral expressing the space part of the exchange interaction matrix element that is given by

$$Z = \int\int \phi_{D^*}(1)\phi_A(2)[e^2/r_{12}]\phi_D(2)\phi_{A^*}(1)\, d\tau_1\, d\tau_2 \tag{10}$$

where r_{12} is the distance between the exchanged elements 1 and 2.

Using hydrogen atom wave functions, Dexter approximated eq 8 by

$$k_{ET} = (2\pi/\hbar)KJ_E \exp(-2R/L) \tag{11}$$

where L is the average van der Waals' radius for the initial and final molecular orbitals of the donor−acceptor system, K is a constant not related to the experimental parameters, and R is the distance between D and A.

The two ET rate constants observed (Table 2) can most readily be interpreted either as one Trp^{109} site that transfers energy to Tb at either the M2 or M3 metal site or two Trp^{109} sites transferring energy to Tb at the M2 and/or M3 metal site by exchange ET through space. A simple calculation based on distance dependence of the ET rate using eq 11 suggests that the expected ratio of the rate constants for ET from Trp^{109} to M3 (the distance being 9.3 Å) and to M2 (the distance being 9.7 Å) is 2, assuming that K, J, and L are of similar magnitude for both the metal sites and taking L as 1 Å.[14] Since in AP the metal-binding sites M2 and M3 are elevated by 7 and 10 deg, respectively, with respect to the center of the indole plane of Trp^{109}, the orientation factor for ET to both metal sites can be taken as the same. M1 is not considered as an acceptor site since it is too far away from the Trp^{109} (the distance being 13.7 Å) to play a significant role as acceptor compared with either M3 or M2. The estimated ratio of 2 is in reasonable agreement with the experimental ratio of 3 found by Schlyer et al.[14] at room temperature. The decay analysis at low temperature, however, suggests that the ratio of the two ET rate constants is ca. 7 at 4.2 and 1.2 K and ca. 11 at 77 K (Table 2). We believe that the higher ratios observed at low temperature are best explained by two distinct Trp^{109} sites acting as donors to either or both metal sites M2 and M3. This contention gains some support from our observation of two conformers/sites of Trp^{109} both in AP and apoAP by ODMR (Figure 4 and Table I). Taking the average distance of Trp^{109} to the Tb site as 9.55 Å, eq 11 then predicts a difference of ca. 1 Å between the distance of Trp^{109} site I and of Trp^{109} site II to Tb at low temperature, assuming only the distance sensitivity of the exchange mech-

anism. However, the orientation factor (orientation of the indole plane in site I and site II with respect to either M2 or M3) could play an important role. The importance of the donor orientation with respect to the acceptor has been observed in several bichromophoric molecules[55] and also in naphthalene-linked crown ether complexes of Eu^{3+}/Tb^{3+},where the lanthanide ion is held noncovalently in a predetermined orientation with respect to the naphthalene π-plane.[56] Our observation of a higher value of the ratio of the two ET rate constants at low temperatures could be due either to a difference of the distance between Trp and Tb sites, a different orientation of Trp^{109} in the two sites with respect to Tb, or both.

Thus, the LTP and the ODMR results presented establish that metal depletion in AP does not perturb the environments of the Trp residues at low temperature. The LTP results suggest further that the environment of Trp^{220} remains unaltered in the Tb-substituted apoAP. Our characterization by LTP and ODMR of the three Trp residues, Trp^{109}, Trp^{220}, and Trp^{268} of AP, apoAP, and TbAP demonstrates that the triplet state of Trp^{109} is involved selectively in ET to Tb in TbAP when Trp is photoexcited to its singlet state. The decay analysis presented suggests that ET occurs primarily by a through-space exchange mechanism. Furthermore, our observation of two distinct sites of Trp^{109} by ODMR in AP and apoAP (not resolvable by LTP) suggests that they each take part in ET, giving rise to time-resolved ET rate constants at low temperature. These results at low temperature, as well as those reported earlier at room temperature[14] demonstrate that ET can occur efficiently from the triplet state of Trp to Tb^{3+} over distances the order of 10 Å. The effective range for ET from the singlet state of aromatic amino acids is considerably shorter.[17,52]

Acknowledgment. This work was partially supported by Grant ES-02662 from the National Institute of Environmental Health Sciences, DHHS. Its contents are solely the responsibility of the authors and do not necessarily reflect the views or policies of NIEHS, DHHS.

References and Notes

(1) Coleman, J. E. *Annu. Rev. Biophys. Biomol. Struct*. **1992**, *21*, 441.
(2) Bosron, W. F.; Anderson, R. A.; Falk, M. C.; Kennedy, F. S.; Vallee, B. L. *Biochemistry* **1977**, *16*, 610.
(3) Hough, E.; Hansen, L. K.; Birknes, B.; Jynge, K.; Hansen, S.; Hordvik, A.; Little, C.; Dodson, E. J.; Derewenda, Z. *Nature* **1989**, *38*, 357.
(4) Volbeda, A.; Lahm, A.; Sakiyama, F.; Suck, D. *EMBO J.* **1991**, *10*, 1607.
(5) Anderson, R. A.; Borson, W. F.; Kennedy, F. S.; Vallee, B. L. *Proc. Natl. Acad. Sci. U.S.A.* **1975**, *72*, 2989.
(6) Tibbitts, T. T.; Murphy, J. E.; Kantrowitz, E. R. *J. Mol. Biol*. **1996**, *257*, 700.
(7) Stec, B.; Holtz, K. M.; Kantrowitz, E. R. *J. Mol. Biol*. **2000**, *299*, 1303.
(8) Schaurte, J. A.; Steel, D. G.; Gafni, A. *Methods Enzymol*. **1997**, *278*, 49.
(9) Vanderkooi, J. M.; Calhoun, D. B.; Englander, S. W. *Science* **1987**, *236*, 568.
(10) Domanus, J.; Strambini, G. B.; Galley, W. C. *Photochem. Photobiol.* **1980**, *31*, 15.
(11) Strambini, G. B.; Gabellieri, E. *Photochem. Photobiol*. **1990**, *51*, 643.
(12) Mersol, J. V.; Steel, D. G.; Gafni, A. *Biochemistry* **1991**, *30*, 668.
(13) Fischer, C. J.; Schauerte, J. A.; Wisser, K. C.; Gafni, A.; Steel, D. G. *Biochemistry* **2000**, *39*, 1455.
(14) Schlyer, B. D.; Steel, D. G.; Gafni, A. *J. Biol. Chem*. **1995**, *270*, 22890.
(15) Cioni, P.; Strambini, G. B.; Degan, P. *J. Photochem. Photobiol., B* **1992**, *13*, 289.
(16) Horrocks, W. D., Jr.; Collier, W. E. *J. Am. Chem. Soc*. **1981**, *103*, 3, 2856.
(17) Bruno, J.; Horrocks, W. D., Jr.; Zauhar, R. J. *Biochemistry* **1992**, *31*, 7016.
(18) Dexter, D. L. *J. Chem. Phys*. **1953**, *21*, 836.
(19) Hogue, C. W.; MacManus, J. P.; Banville, D.; Szabo, A. G. *J. Biol. Chem.* **1992**, *267*, 13340.
(20) Crosby, G. A.; Whan, R. E.; Alire, R. M. *J. Chem. Phys.* **1961**, *34*, 743.
(21) Heller, A.; Wasserman, E. *J. Chem. Phys.* **1965**, *42*, 949.
(22) MacManus, J. P.; Hogue, C. W.; Marsden, B. J.; Sikorska, M.; Szabo, A. G. *J. Biol. Chem.* **1990**, *265*, 10358.
(23) Prendergast, F. G.; Lu, J.; Callahan, P. J. *J. Biol. Chem.* **1983**, *258*, 4075.
(24) Martini, J.-L.; Tetreau, C.; Pochon, F.; Tourvez, H.; Lentz, J.-M.; Lavalette, D. *Eur. J. Biochem.* **1993**, *211*, 467−473.
(25) Hahn, D. K.; Callis, P. R. *J. Phys. Chem. A* **1997**, *101*, 2686.
(26) Galley, W. C.; Purkey, R. M. *Proc. Natl. Acad. Sci. U.S.A.* **1970**, *67*, 1116.
(27) Hershberger, M. V.; Maki, A. H.; Galley, W. C. *Biochemistry* **1980**, *19*, 2204.
(28) Ozarowski, A.; Barry, J. K.; Matthews, K. S.; Maki, A. H. *Biochemistry* **1999,** *38*, 6715.
(29) Kwiram, A. L. In *Triplet State ODMR Spectroscopy. Techniques and Applications to Biophysical Systems*; Clarke, R. H., Ed; Wiley: New York, 1982; p 427.
(30) Maki, A. H. In *Biological Magnetic Resonance*; Berliner, L. J., Reuben, J., Eds.; Plenum: New York, 1984; Vol. 6, p 187.
(31) Hoff, A. J. *Methods Enzymol*. **1994**, *227*, 290.
(32) Maki, A. H. *Methods Enzymol*. **1995**, *246*, 610.
(33) McGlynn, S. P.; Azumi, T.; Kinoshita, M. *Molecular Spectroscopy of the Triplet State*; Prentice Hall: Englewood Cliffs, NJ, 1969.
(34) Ghosh, S.; Misra, A.; Ozarowski, A.; Stuart, C.; Maki, A. H. *Biochemistry* **2001**, *40*, 15024.
(35) Strambini, G. B.; Gonnelli, M. *Biochemistry* **1995**, *34*, 13847.
(36) Schlyer, B. D.; Lau, E.; Maki, A. H. *Biochemistry* **1992**, *31*, 4375.
(37) Wu, J. Q.; Ozarowski, A.; Maki, A. H. *J. Magn. Reson., Ser. A* **1996**, *119*, 82.
(38) Ozarowski, A.; Wu, J. Q.; Maki, A. H. *J. Magn. Reson., Ser. A* **1996**, *121*, 178.
(39) Wu, J. Q.; Ozarowski, A.; Davis, S. K.; Maki, A. H. *J. Phys. Chem*. **1996**, *100*, 11496.
(40) Antheunis, D. A.; Schmidt, J.; van der Waals, J. H. *Chem. Phys. Lett.* **1970**, *6*, 255.
(41) Smith, C. A.; Maki, A. H. *J. Phys. Chem*. **1993**, *97*, 997.
(42) Siegel, M. S. M.S. Thesis, University of California, Davis, CA, 1979.
(43) Anderson, P. W.; Halperin, B. I.; Varma, C. M. *Philos. Mag*. **1972**, *25*, 1.
(44) Phillips, W. A. *J. Low Temp. Phys.* **1972**, *7*, 351.
(45) Gradl, G.; Friedrich, J. *Phys. Rev. B* **1987**, *35***,** 4915.
(46) Simpson, R. T.; Vallee, B. L. *Biochemistry* **1968**, *7*, 4343.
(47) Vallee, B. L.; Auld, D. S. *Biochemistry* **1993**, *32*, 6493.
(48) Dinse, K. P.; Winscom, C. J.; In *Triplet State ODMR Spectroscopy. Techniques and Applications to Biophysical Systems*; Clarke, R. H., Ed.; Wiley: New York, 1982; p 83.
(49) Schlyer, B. D.; Schauerte, J. A.; Steel, D. G.; Gafni, A. *Biophys. J*. **1994**, *67*, 1192.
(50) Livesey, A. K.; Brochon, J. C. *Biophys. J*. **1987**, *52*, 693.
(51) Mathews, K. D.; Bailey-Folkes, S. A.; Kahwa, I. A.; McPherson, G. L.; O'Mahoney, C. A.; Ley, S. V.; Williams, D. J.; Groombridge, C. J.; O'Connor, C. A. *J. Phys. Chem*. **1992**, *96*, 7021.
(52) Horrocks, W. D., Jr.; Sudnick, D. R. *Science* **1979**, *206*, 1194.
(53) Förster, T. *Z. Naturforsch.* **1949**, *5*, 321.
(54) Kirk, W. R.; Wessels, W. S.; Prendergast, F. G. *J. Phys. Chem*. **1993**, *97*, 10326.
(55) Levy, S.-T.; Rubin, M. B.; Speiser, S. *J. Photochem. Photobiol., A* **1992**, *66*, 159.
(56) Bhattacharyya, S.; Sousa, L. R.; Ghosh, S. *Chem. Phys. Lett*. **1998**, *297*, 154.